Int J Adv Manuf Technol (2017) 92:3373–3384
DOI 10.1007/s00170-017-0408-9

ORIGINAL ARTICLE

Development of magnetic abrasive finishing combined with electrolytic process for finishing SUS304 stainless steel plane

Xu Sun[1] · **Yanhua Zou**[1]

Received: 26 September 2016 / Accepted: 5 April 2017 / Published online: 22 April 2017

Abstract This research proposes an effective plane magnetic abrasive finishing (MAF) process which was combined with electrolytic process in order to improve machining efficiency of traditional plane MAF process. The new plane finishing process can make surface of workpiece to be planarized and softened through formed passive films from electrolytic process. Meanwhile, the passive films are removed by magnetic brush-generated mechanical processing force to achieve efficient precision machining. This finishing process is called electrolytic magnetic abrasive finishing (EMAF). In this research, we have developed a novel machining tool of compound magnetic poles and electrodes, which is able to achieve two different processes. The SUS304 stainless steel plane is used as workpiece. In order to select electrolytic finishing time for EMAF process, the investigation of electrolytic process has been carried out before EMAF process. Then, the comparative experiments of EMAF process and MAF process have been conducted in order to investigate the effect of EMAF process. The experimental results show that EMAF process can a little obtain higher quality surface, and machining efficiency is improved by about 50%, which compared with that of traditional plane MAF process. Furthermore, the surface roughness can be reduced to 30.94 nm R_a from original roughness of 393.08 nm R_a in 40 min by the EMAF process.

Keywords Plane magnetic abrasive finishing · Passive films · Electrolytic magnetic abrasive finishing · Compound machining tool · SUS304 plane workpiece · High machining efficiency

✉ Yanhua Zou
yanhua@cc.utsunomiya-u.ac.jp

Xu Sun
dt147111@cc.utsunomiya-u.ac.jp

[1] Graduate School of Engineering, Utsunomiya University, 7-1-2 Yoto, Utsunomiya, Tochigi 321-8585, Japan

1 Introduction

In recent years, many new ultra-precision machining technologies have been developed and used to machine plane workpiece, in which the magnetic abrasive finishing (MAF) process is proven to be an effective precision processing [1–9]. As a precision machining method, the MAF process has been firstly proposed by the Soviet Union engineer Mr. Kargolow [10]. MAF has many advantages in process, such as good flexibility, self-sharpening of magnetic abrasive particles, and easy controllability. Since the 1980s, the MAF processing technology has been researched and conducted by many researchers. Among them, Prof. Shinmura proposed "plane magnetic abrasive finishing process" in which the magnetic pole rotates at a high speed and workpiece is fed [11–13]; Kang and Yamaguchi applied a multiple pole-tip system with alternating magnetic and non-magnetic regions for the internal finishing of long capillary tubes [14]; Lin et al. employed MAF to polish free-form surface of SUS304 material [15]; Yin et al. developed three modes of vibration-assisted MAF process for polishing flat surface and 3D micro-curved surface [16].

Normally, magnetic brush is used to finish workpiece in traditional plane MAF process. Then, in order to obtain high accuracy surface, the micro magnetic abrasive particles need to be used in ultra-precision finishing process. However, there is a serious problem that the hardness of magnetic abrasive particles is softer than the hardness of SUS304 stainless steel [17, 18]. Moreover, the service life of magnetic abrasive

particles is short, if the magnetic abrasive particles cannot promptly be replaced during MAF process, the finishing ability of MAF process will be rather limited [19–21]. Thus, it is difficult for traditional MAF process to achieve both high accuracy surface and machining efficiency.

In order to improve machining efficiency and surface accuracy of MAF mirror-polishing, this study is focused on an effective machining method which is called electrolytic magnetic abrasive finishing (EMAF) process for combining MAF process and electrolytic process in nano-precision mirror-polishing test of the SUS304 plane workpieces [22–24]. It is well known that the SUS304 is a material of poor machinability and non-magnetic. During MAF process, because of that machining pressure of magnetic brush is inadequate, the efficiency of MAF process is low for polishing SUS304 workpiece. Yet, the effects of electrolytic process cannot be affected by hardness of workpiece, and it is suitable for processing most of metallic materials, while the surface of material is dissolved out a lot of ions and carried away by the electrolytic process. Then, the surface hardness of SUS304 may be softened. In other words, the machinability of SUS304 becomes good. Thus, the electrolytic process is taken as primary effect to remove material for the EMAF process [25–30]. Generally, the roughness of metal surface can only reach to less than 200 nm R_a by the electrolytic process. Hence, the MAF process is used to remove the formed passive films from electrolytic process in order to achieve precision machining. If MAF process combines with electrolytic process, the magnetic abrasive could be protected. Moreover, the efficiency of EMAF process is higher than any single process of MAF process or electrolytic process. MAF process and electrolytic process are performed at the same time, but MAF process is adopted as a final process after electrolytic process in order to get a perfect surface profiles accuracy with high machining efficiency. The surface roughness and appearance before processing and after processing are detected by 3D non-contact optical profiling microscopy and measurement scanning electron microscope.

2 Basic machining principle of MAF and EMAF

2.1 Principle of plane MAF process

Figure 1 shows the schematic of traditional "plane MAF polishing process" which is proposed by Prof. Shinmura [31, 32]. The poles are disposed on the top of the workpiece plane. The iron particles are mixed with magnetic abrasive particles and attracted along the magnetic force lines. Then, the magnetic brush is formed on the bottom of the poles. The relative rotation of magnetic pole combines with reciprocating feeding movement of workpiece; a relative friction is produced between surface of workpiece and magnetic brush. The friction is combined with fluctuating magnetic force produced by magnetic brush. Thus, the material removal and surface accuracy of mirror-polishing can be effectively realized.

2.2 Basic processing principle of EMAF

Since the electrolytic process is an important part of EMAF process, principle of electrolytic process will preferentially be introduced in the following. Figure 2 shows the machining principle of electrolytic process. The $NaNO_3$ solution is neutral which produces less pollution for environment. Thus, the $NaNO_3$ solution is adopted as the electrolyte in this study from the view of environmental protection. When turning on DC constant voltage power, aqueous solution of $NaNO_3$ will take place electrolytic reactions which are shown as Eqs. (1) and (2).

$$NaNO_3 \rightarrow Na^{+} + NO^{3-} \quad (1)$$

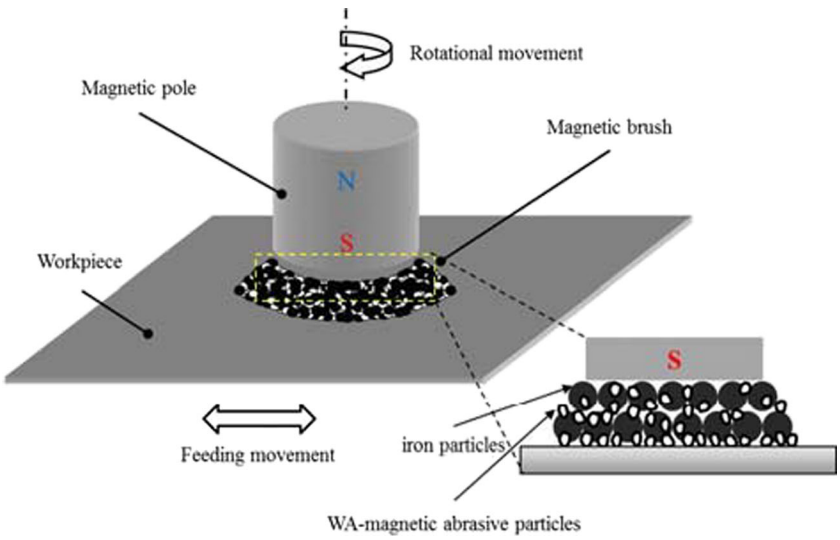

Fig. 1 Schematic of MAF process

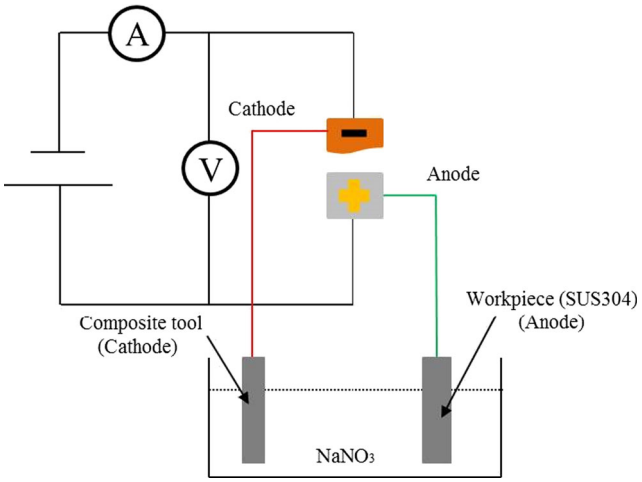

Fig. 2 Schematic of electrolytic process

$$H_2O \rightarrow H^+ + OH^- \quad (2)$$

Na^+ and H^+ move toward the cathode; NO^{3-} and OH^- move toward the anode. Since ionization tendency of "Na" is stronger than ionization tendency of "H," the reaction shown as Eq. (3) occurs at the cathode. The discharge of OH^- is easier than the discharge of NO^{3-}; hence, the reaction shown as Eq. (4) occurs at the anode. Through Eqs. (3) and (4), it can be seen that H_2 is generated at the cathode and O_2 is generated at the anode [33].

$$H^+ + 2e^- \rightarrow H_2\uparrow \quad (3)$$

$$2OH^- \rightarrow H_2O + 1/2O_2\uparrow + 2e^- \quad (4)$$

It is well known that the major composition of SUS304 is Fe (70%), Cr (20%), and Ni (10%). Generated oxygen at the anode has strong oxidizing. Hence, most of anode metal is oxidized under the action of oxygen. Moreover, a lot of mental ions such as Fe^{3+}, Cr^{6+}, Fe^{2+}, Cr^{3+} Ni^{2+}, and other elements are eluted on the metal surface by the action of oxidation reaction [33]. Compared with the concave portions of workpiece, the protruding portions are closer to cathode. Thus, the current density of protruding portions is larger and eluted rate is also relatively faster. These protruding portions of workpiece are preferentially leveled during electrolytic process, and the surface precision polishing can be completed by elution [34, 35]. Along with the electrolytic reaction proceeds, the surface of SUS304 plane will accumulate a large number of passive films which can lead to the electrolytic current gradually to decrease. Thereby, the eluting amount of metal ions will decrease.

The main problem of using MAF process to polish the SUS304 plane is that pressing pressure of magnetic brush is deficiency. However, if the MAF process combines with the electrolytic process, passive films are generated under the action of electrolytic process. Since the hardness of passive films is far lower than that of SUS304 material, magnetic brush can effectively remove formed passive films from the electrolytic process. Thereby, abovementioned, the main problem of using MAF process can be solved, and the machining efficiency can be improved by EMAF process. It is notable that EMAF process includes two finishing steps which are (1st) finishing step (MAF process combines with electrolytic process) and (2nd) finishing step (single MAF process). The schematic of stainless planar processing system is shown as Fig. 3. The SUS304 workpiece as an anode is penetrated into electrolyte solution and connected to positive electrode of DC constant voltage power. The electrolytic magnetic compound machining tool as a cathode is located above the workpiece and connected to negative electrode of DC constant voltage power. There is a working gap between compound machining tool and workpiece plane. The magnetic brush is formed by mixed magnetic abrasive particles at the bottom of the magnetic poles. Then, magnetic brush conducts rotational movement. The electrolyte is injected by a pump and the flow rate of electrolyte is controlled through a flow meter. After turning on DC constant voltage power, the protruding portions will be preferentially leveled and the passive films will form on the surface of workpiece by electrolytic process. At the same time, using the magnetic abrasive particles of magnetic brush to exert friction on the surface of workpiece, the passive films can be effectively removed. Thus, the efficient precision machining of workpiece surface can be realized through EMAF process. In addition, in order to avoid environmental pollution, the used electrolyte is collected into a collecting container.

3 Experimental setup

The electrolytic magnetic compound machining tool has been designed and made before this study, as shown in Fig. 4. In order to achieve that the electric current flows from the power supply to compound machining tool (cathode), a copper ring as a conductor is placed on the top of compound machining tool. The cathode is designed to be cross-shape at the bottom of compound machining tool (two copper rods: 30 × 3 × 3 mm). The magnetic poles are constituted by four circular Nd-Fe-B permanent magnet (four magnetic poles: Φ 6 × 30 mm) and respectively distributed on four directions of the electrodes. In order to avoid short circuit which is caused by connection of magnetic brush and electrode, magnetic poles and electrodes are separated approximately 4 mm.

Figure 5 shows the setup of electrolytic magnetic compound machining experiment. A SUS304 plane with 100 mm in length, 100 mm in width, and 1 mm in thickness is used for the experiments. The SUS304 plane workpiece as an anode is located in the container and connected to the positive of DC constant voltage power. Electrolytic magnetic compound machining tool is fixed on the chuck of milling

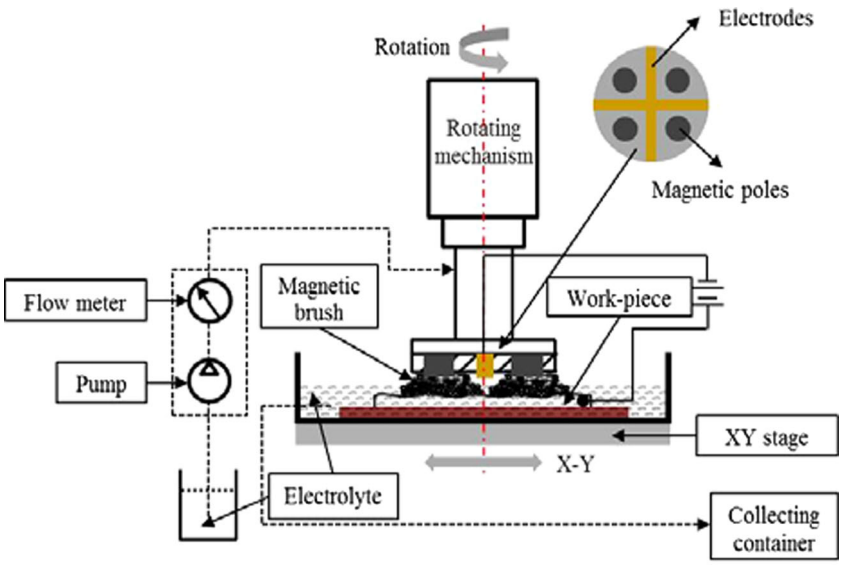

Fig. 3 Schematic of stainless planar process system

machine and placed on the top of SUS304 plane workpiece. The electrodes (copper rods) as a cathode are embedded into bottom of electrolytic magnetic compound machining tool and connected to the negative of DC constant voltage power through a carbon rod and wires. A nozzle is placed near the carbon rod. The electrolyte ($NaNO_3$) is supplied from a nozzle by a pump, and the flow rate of electrolyte is controlled through a flow meter. The plane workpiece and container are laid on the *X*-*Y* stage. The feeding trajectory and velocity of *X*-*Y* stage are controlled by a numerical control (NC) program which has been compiled. When the experiments are performed, a certain working gap is adjusted between workpiece (anode) and compound machining tool (cathode). The magnetic brush is formed by mixing magnetic abrasive grains at the bottom of poles. Then, the electrolytic magnetic compound machining tool performs rotary motion. The rotational direction and velocity of compound machining tool are controlled by milling machine.

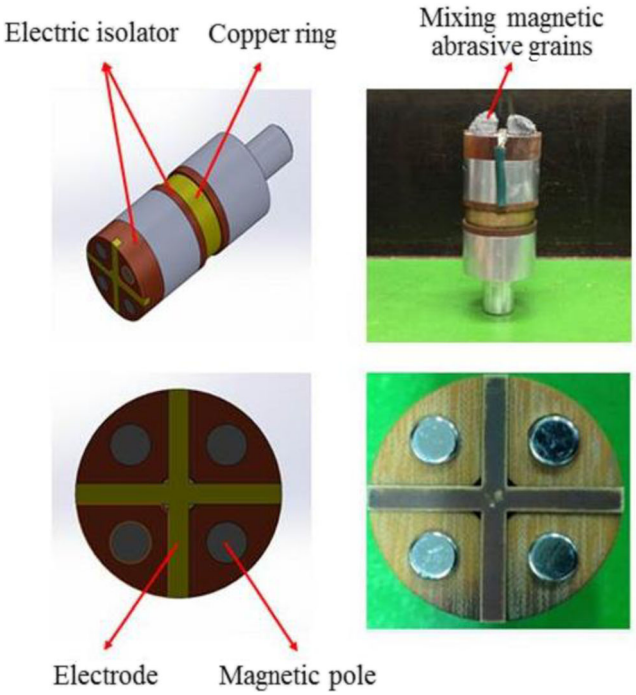

Fig. 4 Schematic and photos of electrolytic magnetic compound machining tool

4 MAF experiments

4.1 Experimental conditions of MAF

In order to compare electrolytic process with EMAF process, the traditional MAF process tests are conducted at room temperature. The detailed experimental conditions of MAF process are shown in Table 1. Surface roughness of workpiece is

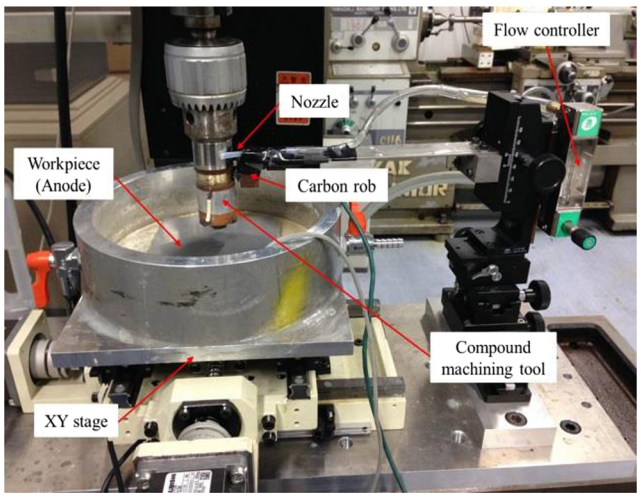

Fig. 5 Photo of experimental setup

measured at approximate 0.39 μm R_a as an original roughness before machining. The finishing time is selected as per 15 min (for six times) to measure and compare the finished surface differences. In order to ensure machining power to be adequate, the working gap is adjusted to 1 mm. For obtaining a higher surface accuracy and higher efficiency, the rotational speed of compound machining tool and feeding speed of *X*-*Y* stage are respectively adjusted to 450 rpm and 5 mm/s [31, 36]. After each step of tests, surfaces of workpiece are observed at nine locations as shown in Fig. 6. The surface roughness of workpiece is measured through a non-contact optical profiling microscope (Wyko Vision NT1100), and the image of finished surface is observed by a scanning electron microscope (HITACHI S4500).

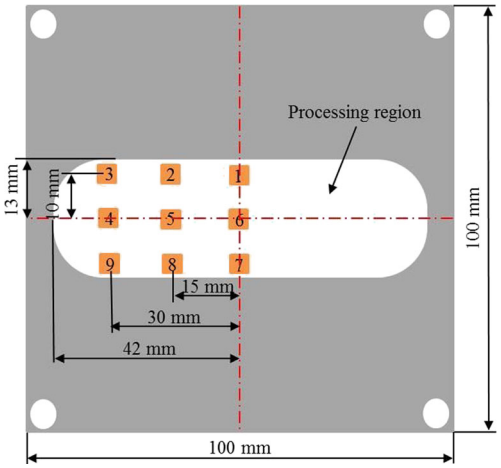

Fig. 6 Observed locations of surface specimen

4.2 Experimental results and discussions of MAF process

Figure 7 shows the non-contact 3D measurement of unfinished surface and finished surface at 75-min traditional MAF process test obtained through a non-contact optical profiling microscope. Compared with the surface profile of original workpiece, it can be clearly seen the change in removal depth h_r at 75-min traditional MAF process, and the surface profile of workpiece almost tends to be planarized.

The SEM photograph of surface before MAF process is shown in Fig. 8a. The initial hairline of surface can be clearly seen through the SEM photograph. Figure 8b shows the SEM photograph of finished surface at 75-min traditional MAF process test obtained by a scanning electron microscope. Compared with the surface of original workpiece, it can be clearly found that the initial hairlines of surface have almost completely been removed. However, just a few concave portions still exist on the surface of workpiece.

In order to quantitatively compare and estimate the difference of surface roughness R_a and material removal weight M under different finishing times of traditional MAF process (per 15 min). The maximum height roughness R_a in the captured field of 299 × 227 μm^2 is estimated using a non-contact optical profiling microscope. The change in material removal weight M is measured through a high-precision electronic scale. Figure 9 shows the change in surface roughness R_a and material removal weight M as a function of MAF process time. The surface roughness R_a is an average surface roughness value of nine observed locations. With finishing time increases, it is noted that the surface roughness remarkably descends from 390.98 nm R_a to 41.49 nm R_a at 75-min MAF process experiment, and then the surface roughness becomes stable after 75-min MAF process test; the material removal weight M continuously keeps increasing during 90-min MAF process test, but the rate of material removal weight M before 30-min MAF process test is more than the rate of material removal weight M after 30-min MAF process test. Since the service life of magnetic abrasive is short and the hardness of magnetic abrasive is relatively soft, it may be the main reason for that the surface roughness R_a becomes stable after 75-min MAF process test and the material removal weight rate before 30-min MAF process test is more than that after 30-min MAF process test.

Table 1 Experimental conditions of MAF process

Conditions of MAF process	
Workpiece	SUS304 plane (100 × 100 × 1 mm)
Original roughness	0.39 μm R_a
Compound magnetic abrasives	Electrolytic iron powder (149, 75, and 30 μm in mean diameter) WA particles: #800, #4000, #8000, #10000 Oily grinding fluid
Working gap	1 mm
Stage feeding speed	5 mm/s
Tool rotational speed	450 rpm
MAF test time	90 min

5 EMAF experiment

5.1 Experimental conditions of electrolytic process

By the foregoing narrative, it is easy to see that electrolytic process plays an extremely important role during EMAF process. Therefore, the investigation of electrolytic process is carried out before EMAF process. Table 2 describes experimental conditions of electrolytic process. Because finished surface roughness during electrolytic process generally can reach to below 0.2 μm R_a, the original surface roughness of workpiece is selected as approximately 0.39 μm R_a before machining. The working gap is adjusted to 1 mm in order to ensure processing effect. The rotational speed of compound

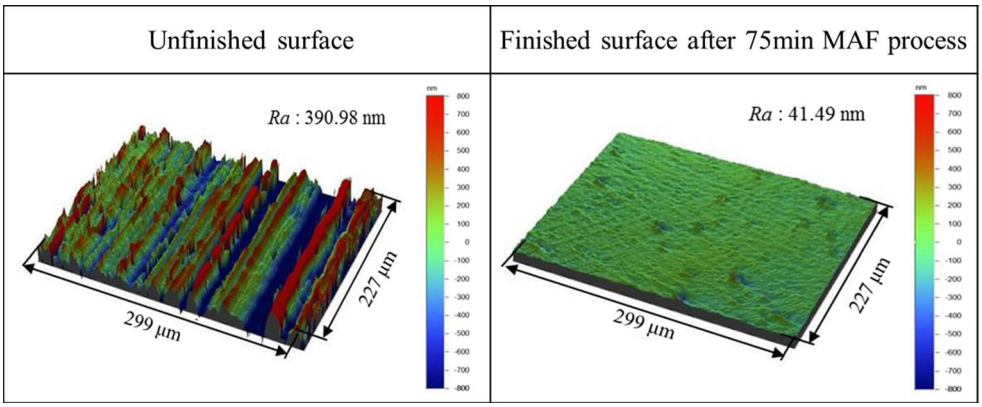

Fig. 7 Non-contact 3D measurement of unfinished surface and finished surface after 75-min MAF process

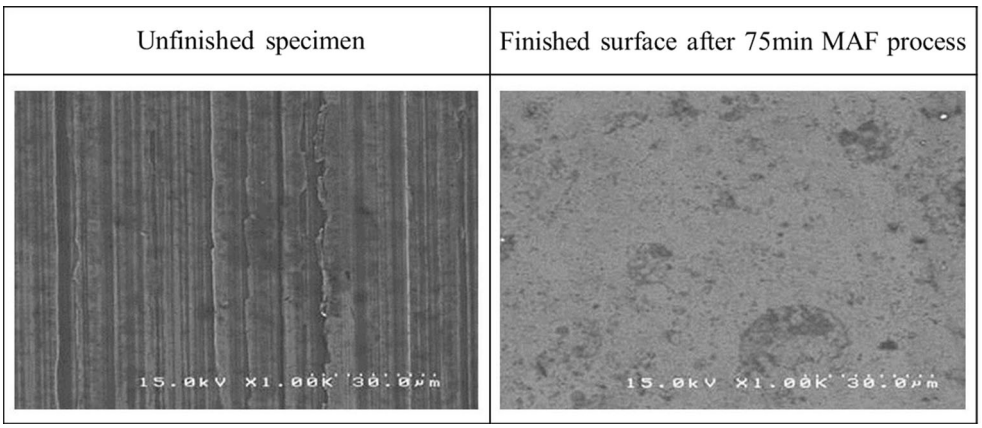

Fig. 8 SEM images of unfinished surface and finished surface after 75-min MAF process

machining tool and feeding speed of *X-Y* stage are respectively adjusted to 450 rpm and 5 mm/s. The main feature of electrolytic process is that processing speed can be accelerated. Thereby, the total finishing time is selected as 10 min, and the finished surface is measured at per 2 min. The 20 wt% sodium nitrate is adopted as the electrolyte. The flow rate of electrolyte is adjusted to 300 ml/min. Electrical current is set as 2.5 A through an 8 V DC constant voltage. The value of working current can influence current density which can be calculated by Eq. (5). In other words, the current density can indirectly be controlled by voltage applied to electrodes.

$$J = I / A, \tag{5}$$

where "J" is current density, "I" is electrolytic current, and "A" is area of cathode. Thus, it can be found that the current density "J" as an important parameter of electrolytic process is proportional to the electrolytic current "I" and inversely proportional to the area of cathode "A" through Eq. (5). After each step of electrolytic process experiment, the surface roughness of workpiece is measured through a non-contact

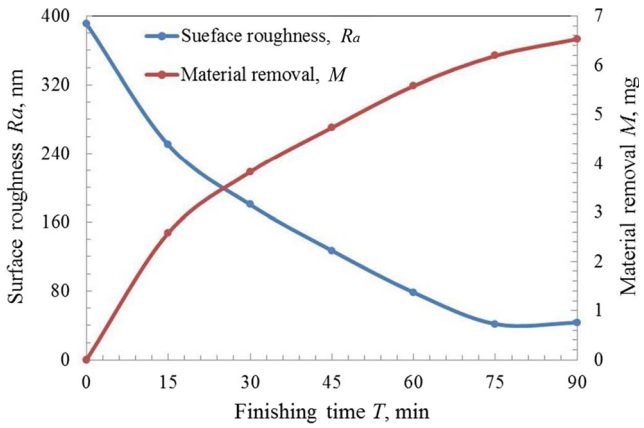

Fig. 9 Change in surface roughness Ra and material removal M as a function of MAF processing time

Table 2 Experimental conditions of electrolytic process

Conditions of electrolytic process	
Workpiece	SUS304 plane (100 × 100 × 1 mm)
Original roughness	0.39 μm R_a
Working gap	1 mm
Stage feeding speed	5 mm/s
Tool rotational speed	450 rpm
Working voltage	8 V
Electrolyte	$NaNO_3$ (20 wt%)
Flow rate	300 ml/min
Electrolytic test time	10 min

optical profiling microscope; the images of finished surface are observed by a scanning electron microscope.

5.2 Experimental results and discussions of electrolytic process

Figure 10 shows a series of SEM photographs of surface before the electrolytic process and after the electrolytic process. The initial hairline of unfinished surface can be clearly seen through the SEM photograph (1000 times) of Fig. 10a. Figure 10b~f respectively shows the SEM photographs (1000 times) of finished surface at 2-, 4-, 6-, 8-, and 10-min electrolytic process experiment obtained by a scanning electron microscope. Compared with the surface of workpiece before machining, it can be clearly found that the initial hairlines of surface have been almost completely removed. However, a lot of micro-porous generate on the surface of workpiece. Furthermore, under the action of electrolytic process, the number of micro-porous increases with the finishing time increases; the size of micro-porous becomes small with the finishing time increases, and the depth of micro-porous also deepens.

In order to investigate the optimal parameters of electrolytic process, the differences of surface roughness R_a and material removal weight M have been quantitatively compared and estimated at different finishing time of electrolytic process (per 2 min). Figure 11 shows the change in surface roughness R_a and material removal weight M at different finishing times of electrolytic process. With the finishing time increases, it is noted that the surface roughness remarkably descends from 394.81 to 160.03 nm R_a at 4-min finishing time of electrolytic process, and then the surface roughness R_a increases when the finishing time of electrolytic process is more than 4 min; the material removal weight M continuously keeps increasing during 10-min electrolytic process test, but the rate of material removal weight M before 4-min electrolytic process test is higher than that after 4-min electrolytic process test. After the action of electrolytic process, the surface of SUS304 plane will accumulate a large number of passive films which can make the electrolytic current gradually to decrease, and then the eluting amount of metal ions will decrease. It may be the main reason for that the surface roughness R_a increases after 4-min electrolytic process test, and the rate of material removal weight M before 4-min electrolytic process test is higher than the rate of material removal weight M after 4-min electrolytic process test.

5.3 Experimental conditions of EMAF

The EMAF process step is conducted in one step simultaneously for combining electrolytic process and MAF process. Although the surface can be leveled through electrolytic process, generated passive films by the action of electrolytic process will affect the accuracy of surface. Thus, in order to completely remove passive films, electrolytic process has to be stopped before MAF process. Since over a long period electrolytic process can lead to the formed passive films thicken, the finishing time of EMAF process step is selected as 4 min. After EMAF process, electrolytic process is stopped and MAF process continues to be conducted for 41 min. The total EMAF finishing time is selected as 4, 15, 25, 35, 40, and 45 min to observe and compare the difference of polishing surfaces during different steps of MAF process. The detailed experimental conditions of EMAF are shown in Table 3. The

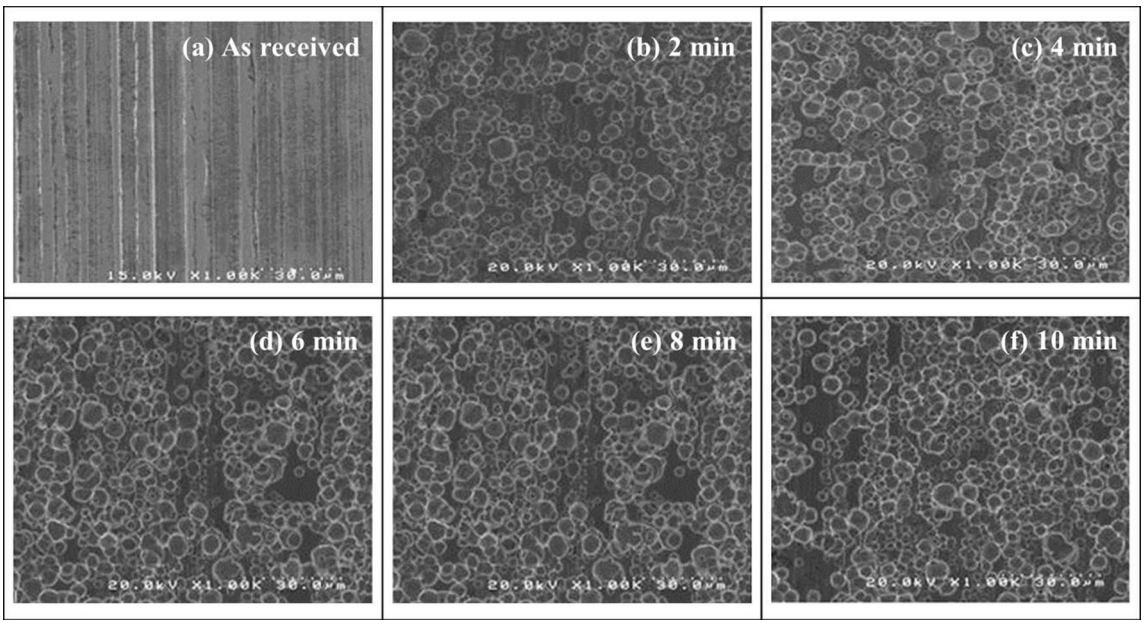

Fig. 10 Macroscopic confocal images of unfinished surface and finished surface in various conditions after 2-, 4-, 6-, 8-, and 10-min experiments

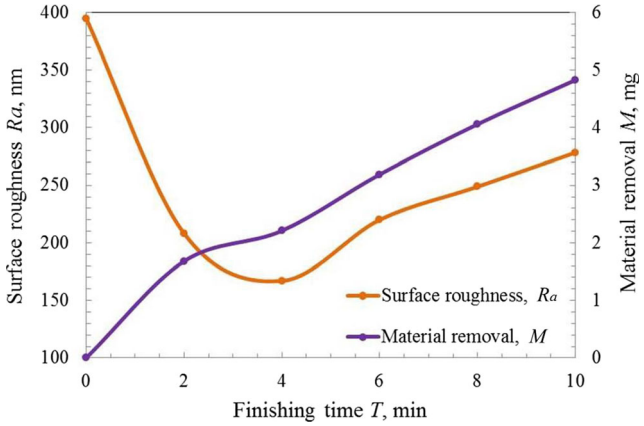

Fig. 11 Change in surface roughness R_a and material removal M as a function of electrolytic processing time

sodium nitrate 20 wt% is used as electrolyte and flows at 300 ml/min. Electrolytic current is set as 2.5 A through an 8 V DC constant voltage. According to Eq. (5), the current density can be indirectly controlled by voltage applied to electrodes. After each step of EMAF process tests, surface roughness R_a of workpiece is measured through a non-contact optical profiling microscope; the image of finished surface is observed by a scanning electron microscope.

5.4 Experimental results and discussions of EMAF process

Figure 12 shows the non-contact 3D measurement of finished surface at 45-min EMAF process experiment (it includes 4-min EMAF process and 41-min MAF process) obtained through a non-contact optical profiling microscope. Compared with the surface profile of workpiece before machining, it can be clearly seen the change in removal depth h_r at 45-min EMAF process, and the surface profile of workpiece tends to be planarized. Furthermore, compared with the surface profile of workpiece during traditional MAF process, it can be obviously found that the surface roughness R_a of EMAF process is a little better than the surface roughness R_a of traditional MAF process.

Table 3 Experimental conditions of EMAF process

Conditions of EMAF process	
Workpiece	SUS304 plane (100 × 100 × 1 mm)
Original roughness	0.39 μm R_a
Compound magnetic abrasives	Electrolytic iron powder (149, 75, and 30 μm in mean diameter) WA particles #800, #4000, #8000, #10000 Oily grinding fluid
Working gap	1 mm
Stage feeding speed	5 mm/s
Tool rotational speed	450 rpm
Working voltage	8 V
Electrolyte	$NaNO_3$ (20 wt%)
Flow rate	300 ml/min
EMAF test time	4 min (EMAF) + 41 min (MAF)

The SEM photograph of original surface before EMAF process is shown in Fig. 13a. The initial hairline of unfinished surface can be clearly seen through the SEM photograph. Figure 13b shows the SEM photograph of finished surface after the first finishing step (4-min EMAF process). It can be seen that a small amount of micro-porous still exists on the finished surface through the SEM photograph. Moreover, it also indicates that when two kinds of finishing processes simultaneously are executed, the action of MAF process can not completely remove the generated passive films from electrolytic process. The SEM photograph of finished surface after the second finishing step (41-min MAF process) is shown in Fig. 13c. Compared with the original surface of workpiece, it can be clearly found that the initial hairline of surface has been almost completely removed. Furthermore, it also can be confirmed that MAF process plays an essential role during the EMAF process.

Figure 14 shows the change in surface roughness R_a and material removal weight M under different finishing times of EMAF process. The measurement of change in surface roughness R_a is operated through a non-contact optical profiling microscope. With the finishing time increases, the surface roughness descends from original surface roughness 393.08 to 268.44 nm R_a after the first finishing step (EMAF process), and then the surface roughness continues to descend from 268.44 to 31.58 nm R_a after the second finishing step (single MAF process). It is noted that the surface roughness firstly descends from 393.08 to 30.94 nm R_a at 40-min EMAF process test, and then the surface roughness R_a becomes stable after 40-min EMAF process test. The change in material removal weight M is measured through a high-precision electronic scale. The material removal weight M markedly continues to increase with the finishing time increases, but the rate of material removal weight M during the first finishing step (4-min EMAF process) is obviously higher than the rate of material removal weight M during the second finishing step (41-min MAF process). Moreover, compared with the material removal rate of single MAF process, the material removal rate of EMAF process step is nearly three times than that of single MAF process step. Then, the change in surface roughness R_a is mainly caused by EMAF process itself. The removal depth h_r can be calculated by the following Eq. (6).

$$hr = m / A_p \rho, \tag{6}$$

where "m" is mass of material removal, "A_p" is working area, and "ρ" is density of material. According to the result of material removal weight M shown in Fig. 14, the removal depth h_r ranged from 0 to 2.4 μm. Yet, the surface roughness R_a has little change when finishing time is more than 40 min. It is

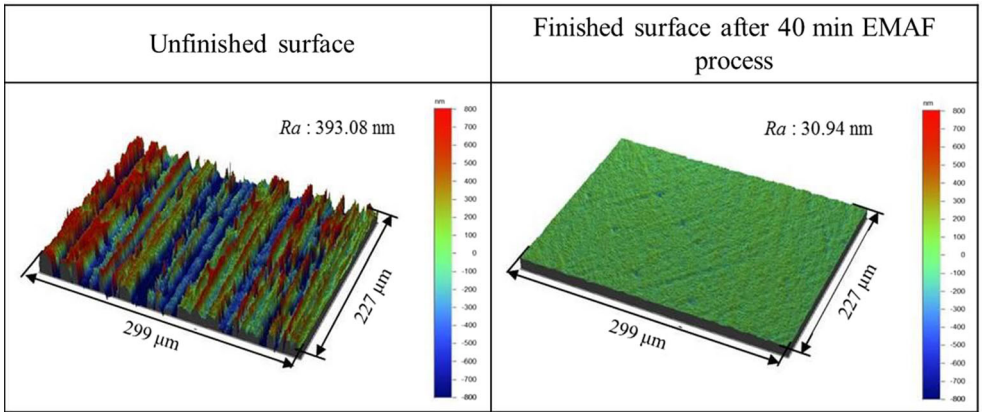

Fig. 12 Non-contact 3D measurement of unfinished surface and finished surface after 40-min EMAF process

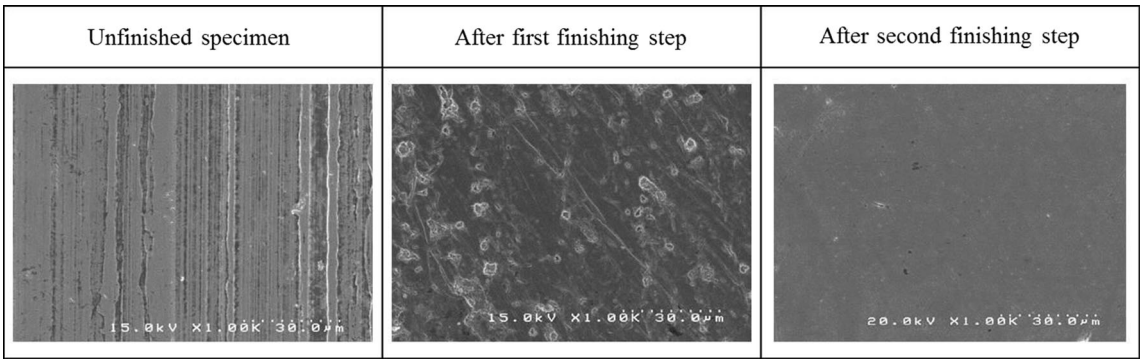

Fig. 13 Macroscopic confocal images of unfinished surface and finished surface in various conditions after the first finishing step and second finishing step experiments

probably because removal depth h_r is larger than the value of original roughness. Moreover, the effects of electrolytic process and magnetic abrasive have reached to finishing balance. Therefore, the surface roughness no longer declines. During the EMAF process, a large amount of metal ions dissociate from the surface of workpiece. Thus, the rate of material removal weight M before 4-min EMAF process (EMAF process step) is higher than the rate of material removal weight M after 4-min EMAF process test (single MAF process step).

Finally, the comparison of EMAF process and MAF process is shown in Fig.15. It is recognized that the material removal efficiency of EMAF process is remarkably higher than that of traditional MAF process, and the surface quality of EMAF process is a little better than that of MAF process. Therefore,

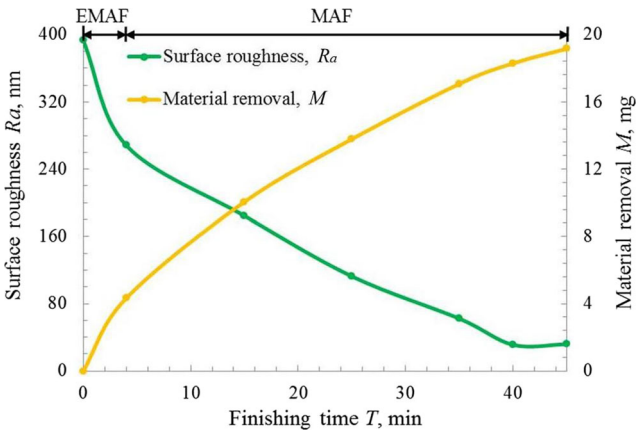

Fig. 14 Change in surface roughness R_a and material removal M as a function of EMAF processing time

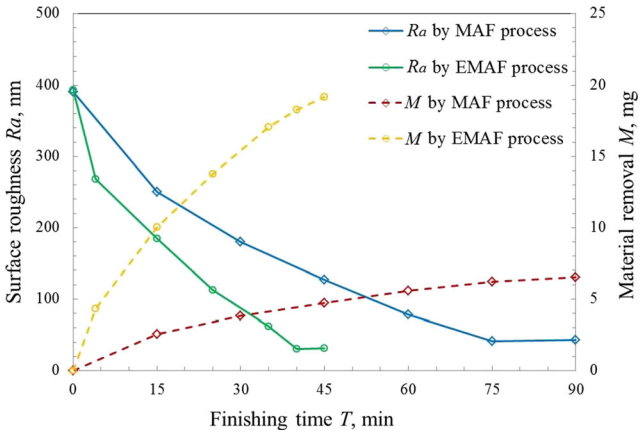

Fig. 15 The comparison of EMAF process and MAF process for surface roughness R_a and material removal M

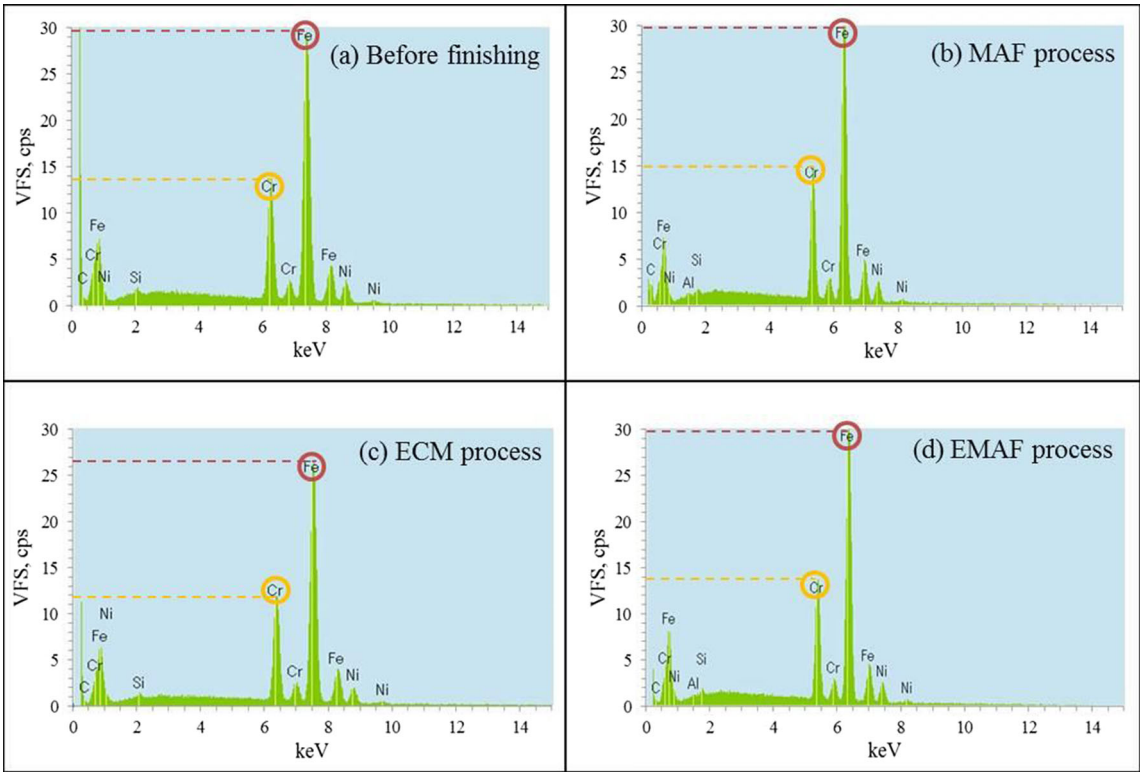

Fig. 16 EDX analysis of unfinished surface and finished surface by different machining processes

this new finishing process can be proven to more efficiently polish SUS304 plane than the traditional MAF process.

6 EDX analysis of surface composition

The homogeneity of finished surface materials as an important parameter is investigated by energy-dispersive X-ray spectroscopy (HITACHI S 4500 & HITACHI TM 3030 Plus) to evaluate the change in elemental composition during different finishing processes. Figure 16 shows the energy-dispersive X-ray (EDX) of finished surface after different finishing processes. The composition of original surface is shown in Fig. 16a. It can be confirmed that the major composition of SUS304 is constituted by Fe, Cr, Ni, and other elements through Fig. 16a. Figure 16b~d respectively shows that composition of finished surface through MAF process, electrolytic process, and EMAF process. Compared with the composition of original

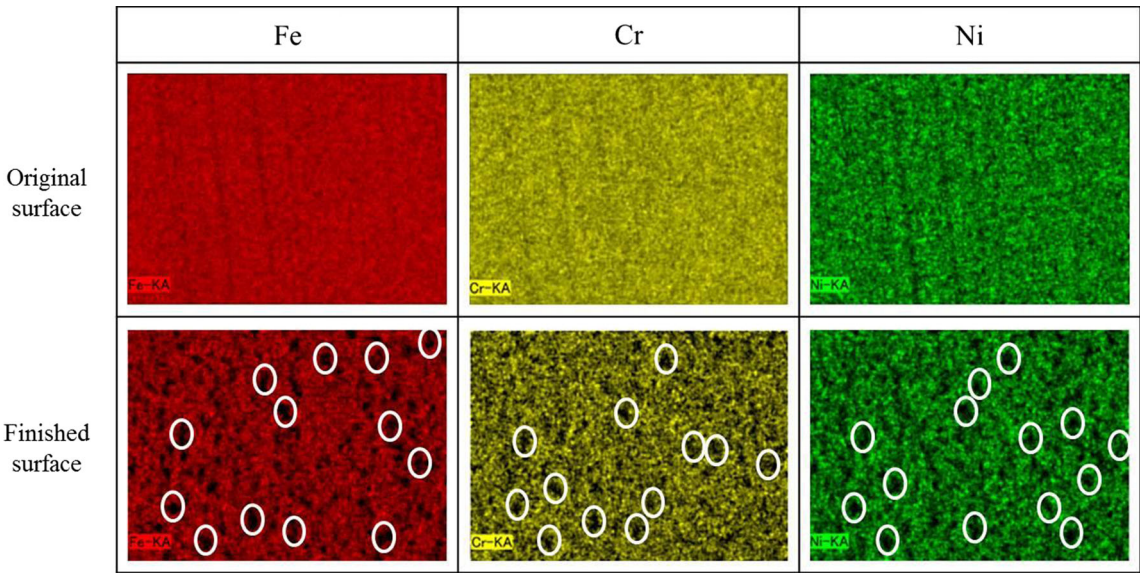

Fig. 17 Representative SEM images and elemental mapping of Fe, Cr, and Ni elements

surface, it can be found that the composition of finished surface by MAF process and the composition of finished surface by EMAF process are similar to the composition of original surface. During the MAF process, the workpiece surface is processed by mechanical stress; thus, the composition of machined surface is not any change. Through comparing Fig. 16a and Fig. 16d, it can be revealed that the formed passive films have been almost completely removed during the total EMAF process; then, the original material exposes on the surface. However, Fig. 16c shows that the composition of finished surface through electrolytic process is significantly different from the composition of original surface. As previously mentioned, a large amount of metal ions have been dissolved out on the surface of the workpiece under the action of electrolytic process. Moreover, the eluted elements such as Fe^{3+}, Cr^{6+}, Fe^{2+}, Cr^{3+}, and Ni^{+2} combine with OH^- (Eq. (2)); the $Fe(OH)_3$, $Fe(OH)_2$, $Cr(OH)_6$, $Cr(OH)_3$, and $Ni(OH)_2$ precipitate to be generated in the electrolyte [33]. It is the main reason for that the content of Fe, Cr, and Ni elements during electrolytic process is less than the content of original surface composition.

Obviously, it can be confirmed that the electrolytic process is a main reason for leading to change in the content of finished surface composition. Since the major composition of SUS304 material is constituted by Fe, Cr, and Ni elements; thus, Fig. 17 depicts some representative images of Fe, Cr, and Ni elements along with the local elemental distribution mapping. The main compositions of original surface before electrolytic process are shown in Fig. 17a; the change in main compositions of the finished surface after electrolytic process is shown in Fig. 17b. By comparing the analysis results, it can be revealed that a lot of large black dots which cannot be identified substance shown in white circle inner generates on the finished surface, and the content of each element significantly decreases during electrolytic process. The results also completely conforms that electrochemical reactions occur during the electrolytic process. In addition, the local elemental mapping indicates that the distribution of Fe, Cr, and Ni elements becomes non-uniform after electrolytic process.

7 Conclusion

This paper proposed plane magnetic abrasive finishing combined with the electrolytic process, which is used to finishing SUS304 stainless steel plane. The main conclusions are summarized as follows:

1. The proposed plane magnetic abrasive finishing combined with the electrolytic process method has successfully achieved efficient precision machining. Additionally, a novel designed electrolytic magnetic compound machining tool has been successfully applied in EMAF process tests to simultaneously achieve two different processes (MAF process and electrolytic process).

2. The results of experiments show that the surface roughness can reach to 41.49 from 390.98 nm R_a by 75-min traditional MAF process; the surface roughness descends from 393.08 to 30.94 nm R_a by 40-min EMAF process.

3. The results of EDX analysis have revealed that the electrolytic process is regarded as the main effect for the change in content of surface composition and soften surface during the EMAF process. Since the electrolytic magnetic abrasive finishing can soften the surface of workpiece, the material removal weight M of total EMAF process is nearly six times than that of single traditional MAF process.

4. Through contrasting with traditional MAF process, it is confirmed that EMAF process can a little obtain higher quality surface, and machining efficiency is improved by about 50%.

Acknowledgments We acknowledge valuable contributions and support from the Utsunomiya University Creative Department for Innovation (CDI). We also acknowledge partial contribution from graduates Mr. Longjian Piao (now working in Tomoekogyo Company) for this study.

References

1. Kim TW, Kang DM, Kwak JS (2010) Application of magnetic abrasive polishing to composite materials. J Mech Sci Technol 24:1029–1034
2. Singh DK, Jain V, Raghuram V (2006) Experimental investigations into forces acting during a magnetic abrasive finishing process. Int J Adv Manuf Technol 30:652–662
3. Kim JD, Choi MS (1995) Simulation for the prediction of surface-accuracy in magnetic abrasive machining. J Mater Process Technol 53:630–642
4. Fox M, Agrawal K, Shinmura T, Komanduri R (1994) Magnetic abrasive finishing of rollers. CIRP Annals-Manufacturing Technology 43:181–184
5. Shinmura T, Takazawa K, Hatano E, Matsunaga M (1990) Study on magnetic abrasive finishing. Ann CIRP 39(l):325–328
6. Ihar I, Nakano E, McLamore E, Schueller JK, Toyoda K, Umetsu K, Yamaguchi H (2017) Cleanability of milk deposits on inner stainless steel tubing surfaces prepared by magnetic abrasive finishing. Int Journal of Engineering in Agriculture, Environment and Food 10(Issue 1):63–68
7. Kala P, Sharma V, Pandey PM (2017) Surface roughness modelling for double disk magnetic abrasive finishing process. J Manuf Process 25:37–48
8. Hashimoto F, Yamaguchi H, Krajnik P, Wegener K, Chaudhari R, Hoffmeister H-W, Kuster F (2016) Abrasive fine-finishing technology. CIRP Ann Manuf Technol 65:597–620
9. Yamaguchi H, Srivastava AK, Tan M, Hashimoto F (2014) Magnetic abrasive finishing of cutting tools for high-speed machining of titanium alloys. CIRP J Manuf Sci Technol 7:299–304
10. Lijun XU, Wen WANG, Cheng YANG (2003) Review of magnetic abrasive finishing (application to plane finishing), China Academic Journal Electronic Publish House 1001–2265 01–0041–03
11. Shinmura T, Takazawa K, Hatano E (1985) Study on magnetic abrasive process (application to plane finishing). Bull of the JSPE 19(4):289–294

12. Shinmura T, Aizawa T (1988) Development of plane magnetic abrasive inishing apparatus and its finishing performance (2nd report, finishing apparatus using a stationary type electromagnet). J. Jpn. Soc. Prec. Eng. 54(5):928–933 **(in Japanese)**
13. Yanhua Zou, Anyuan Jiao, Toshio Aizawa, 2010 Study on plane magnetic abrasive finishing process-experimental and theoretical analysis on polishing trajectory. Advanced Materials Research., Vol.126–128, pp:1023–1028
14. Kang J, Yamaguchi H (2012) Internal finishing of capillary tubes by magnetic abrasive finishing using a multiple pole-tip system. Precis Eng 36(3):510–516
15. Lin CT, Yang LD, Chow HM (2007) Study of magnetic abrasive finishing in free-form surface operations using the Taguchi method. Int J Adv Manuf Technol 34(1–2):122–130
16. Yin S, Shinmura T (2004) Vertical vibration-assisted magnetic abrasive finishing and deburring for magnesium alloy. Int J Mach Tools Manuf 44:1297–1303
17. Zhu Y-J, Ding W-F, Xu J-H, Yu-Can F (February 2015) Surface fractal evolution of fracture behavior of polycrystalline cBN grains in high-speed grinding. Int J Adv Manuf Technol 76(Issue 9):1505–1513
18. John Wiley & Sons, Chichester. Micro cutting: fundamentals and applications. October 2013. ISBN: 9780470972878
19. GY Liu, ZN Guo, SZ Jiang, NS Qu, YB Li (2014) A study of processing Al 6061 with electrochemical magnetic abrasive finishing. 6th CIRP International Conference on High Performance Cutting, HPC2014. Procedia CIRP 14 234–238
20. KIM SO, KWAK JS (2008) Magnetic force improvement and parameter optimization for magnetic abrasive polishing of AZ31 magnesium alloy. Trans Nonferrous Met Soc China 18:s369–s373
21. Sankar MR, Ramkumar J, Jain VK (2009) Experimental investigation and mechanism of material removal in nano finishing of MMCs using abrasive flow finishing (AFF) process. Wear 266: 688–698
22. KWAK TS, LEE YC, ANZAI M, OHMORI H (2005) Study on nano-level mirror surface finishing using ELID grinding and magnetic abrasive finishing. J of Japan Society for Abrasive Technology 49(2):95–97
23. KWAK TS, KIM GN, LEE YC (2006) Study on nano-level mirror surface finishing on mold core to glass lens molding. J of KSPE 23(1):97–104
24. Yanhua Zou, Longjian Piao (2014) Research on electrolytic magnetic abrasive finishing method. Engineering society academic lecture (spring meeting), Tokyo
25. Pa P (2009) Super finishing with ultrasonic and magnetic assistance in electrochemical micro-machining. Electrochemical Acta 54: 6022–6027
26. Fang J, Jin Z, Xu W, Shi Y (2002) Magnetic electrochemical finishing machining. J Mater Process Technol 129:283–287
27. Kim JD, Xu YM, Kang YH (1998) Study on the characteristics of magneto-electrolytic-abrasive polishing by using the newly developed nonwoven-abrasive pads. Int J Mach Tools Manuf 38:1031–1043
28. Strehblow HH (2003) Passivity of metals. Adv Electrochem Sci Eng 8:271–374
29. Hang W, Zhou L, Zhang K, Shimizu J, Yuan J (Apr. 2016) Study on grinding of $LiTaO_3$wafer using effective cooling and electrolyte solution. Journal of the International Societies for Precision Engineering and Nanotechnology 44:62–69
30. Ridha MM, Zou Y, Sugiyama H (2015) Development of a new internal finishing of tube by magnetic abrasive finishing process combined with electrochemical machining. International Journal of Mechanical Engineering and Applications 3:22–29
31. Shinmura T (1989) Study on plane magnetic abrasive finishing (3rd report on the finishing characteristics of non-ferromagnetic substance). J Jpn Soc Prec Eng 55(7):1271–1276 **(in Japanese)**
32. Shinmura T (1986) Study on free-form surface finishing by magnetic abrasive finishing process (1st report, fundamental experiments). Trans Jpn Soc Mech Eng 53(485C):202–208 **(in Japanese)**
33. Yasuo Kimoto (1994) Ultra-precision machining by electrolytic complex method. Tokyo:aipishi: P111–116
34. Lin TR, Su CR (2008) Experimental study of lapping and electropolishing of tungsten carbides. Int J Adv Manuf Technol 36(7–8):715–723
35. Lee ES (2000) Machining characteristics of the electropolishing of stainless steel (STS316L). Int J Adv Manuf Technol 16(8):591–599
36. T. Shinmura, K. Takazawa, E. Hatano (1985) Study on magnetic abrasive process-finishing characteristics. Vol. 19, No.1 54